



ELSEVIER

Contents lists available at ScienceDirect

## Continental Shelf Research

journal homepage: [www.elsevier.com/locate/csr](http://www.elsevier.com/locate/csr)

## Research papers

## The plankton community in Norwegian coastal waters—abundance, composition, spatial distribution and diel variation

Gunnar Bratbak<sup>a,\*</sup>, Stéphan Jacquet<sup>b</sup>, Aud Larsen<sup>c</sup>, Lasse H. Pettersson<sup>d</sup>, Andrey F. Sazhin<sup>e</sup>, Runar Thyrhaug<sup>a,1</sup><sup>a</sup> Department of Biology, University of Bergen, P.O. Box 7800, N-5020 Bergen, Norway<sup>b</sup> INRA, UMR CARTELE, 75 avenue de Corzent, 74200 Thonon-les-Bains, France<sup>c</sup> Uni environment, Uni Research, Thormøhlens gate 49 B, N-5006 Bergen, Norway<sup>d</sup> Nansen Environmental and Remote Sensing Center, Thormøhlens gate 47, N-5006 Bergen, Norway<sup>e</sup> P.P. Shirshov Institute of Oceanology RAS, 36 Nakhimovskiy Prospect, Moscow 117997, Russia

## ARTICLE INFO

## Article history:

Received 15 September 2010

Received in revised form

15 June 2011

Accepted 26 June 2011

## Keywords:

Phytoplankton

Virus

Diversity

Remote sensing

Ocean color

Skagerrak

## ABSTRACT

The purpose of the present study was to explore the composition and variation of the pico-, nano- and micro-plankton communities in Norwegian coastal waters and Skagerrak, and the co-occurrence of bacteria and viruses. Samples were collected along three cruise transects from Jæren, Lista and Oksøy on the south coast of Norway and into the North Sea and Skagerrak. We also followed a drifting buoy for 55 h in Skagerrak in order to observe diel variations. Satellite ocean color images (SeaWiFS) of the chlorophyll *a* (chl *a*) distribution compared favorably to *in situ* measurements in open waters, while closer to the shore remote sensing chl *a* data was overestimated compared to the *in situ* data. Using light microscopy, we identified 49 micro- and 15 nanoplankton sized phototrophic forms as well as 40 micro- and 12 nanoplankton sized heterotrophic forms. The only picoeukaryote (0.2–2.0 μm) we identified was *Resultor micron* (Pedinophyceae). Along the transects a significant variation in the distribution and abundance of different plankton forms were observed, with *Synechococcus* spp and autotrophic picoeukaryotes as the most notable examples. There was no correlation between viruses and chl *a*, but between viruses and bacteria, and between viruses and some of the phytoplankton groups, especially the picoeukaryotes. Moreover, there was a negative correlation between nutrients and small viruses (Low Fluorescent Viruses) but a positive correlation between nutrients and large viruses (High Fluorescent Viruses). The abundance of autotrophic picoplankton, bacteria and viruses showed a diel variation in surface waters with higher values around noon and late at night and lower values in the evening. *Synechococcus* spp were found at 20 m depth 25–45 nautical miles from shore apparently forming a bloom that stretched out for more than 100 nautical miles from Skagerrak and up the south west coast of Norway. The different methods used for assessing abundance, distribution and diversity of microorganisms yielded complementary information about the plankton community. Flow cytometry enabled us to map the distribution of the smaller phytoplankton forms, bacteria and viruses in more detail than has been possible before but detection and quantification of specific forms (genus or species) still requires taxonomic skills, molecular analysis or both.

© 2011 Elsevier Ltd. All rights reserved.

## 1. Introduction

The phytoplankton in the North Sea, Skagerrak and the adjacent coastal waters have been studied for more than a century (for review see Reid et al., 1990). The focus of these investigations and the approaches as well as the methods used to study and understand the plankton community in the sea has of course changed

considerably over the years. The focus has changed from the taxonomic inventory of the plankton community to a system approach with bulk phytoplankton measurements and biomass budgets where the aim has been to understand the role of phytoplankton as a functional group in the food web. The early studies applied plankton nets with mesh size of 50 or 20 μm while later studies have recognized the importance of the smaller forms passing such nets. The methods applied range from light microscopy observations of single samples to large scale surveys using continuous plankton recorders or quantitative satellite remote sensing. Use of electron microscopy, and epifluorescence microscopy and flow cytometry in combination with high yield fluorescent dyes

\* Corresponding author. Tel.: +47 55 58 2658; fax: +47 55 58 4450.

E-mail address: Gunnar.Bratbak@bio.uib.no (G. Bratbak).

<sup>1</sup> Deceased.

have promoted the discovery and investigation of the smallest members of the plankton community including the role of picophytoplankton, bacteria and viruses. Furthermore, molecular techniques have allowed us to examine the composition of microbial communities and populations at different taxonomic resolution and even below the species level. Recognition of the ecological importance of biodiversity in general and introduction of molecular methods in microbial ecology are perhaps the main factors leading to a renewed interest in the taxonomic inventory of plankton communities.

The community composition of larger phytoplankton forms and the general pattern of seasonal succession in Norwegian coastal waters are well known and described in the literature (e.g. Braarud et al., 1958; Braarud and Nygaard, 1980; Erga and Heimdal, 1984; Lange et al., 1992; Dahl and Johannessen, 1998). Typically, a winter-spring diatom bloom dominated by *Skeletonema*, *Chaetoceros* spp and *Thalassiosira* spp. is succeeded by dinoflagellates and haptophytes including *Ceratium*, *Gyrodinium* and *Gymnodinium* species, *Emiliana huxleyi* and *Phaeocystis pouchetii* in spring-summer. Less is, however, known about the occurrence of the smaller phytoplankton species, i.e. nano- and pico-plankton. The main reasons for this are that many of these are naked and delicate forms that are difficult to preserve with fixatives and that they in addition are difficult to recognize or impossible to identify by light microscopy alone. In an extensive study of flagellates from Norwegian coastal waters, 79 autotrophic and heterotrophic flagellate species have been recorded (Throndsen, 1969), and from one station at the south coast of Norway, 54 species, including 17 Prymnesiophyceae, 13 Chrysophyceae, 6 Prasinophyceae and 18 Choanoflagellida were observed (Espeland and Throndsen, 1986). The culture technique used in these studies is selective and the recorded diversity is presumably grossly underestimated (Throndsen, 1969). The most abundant forms observed include *Micromonas pusilla*, *Nephroselmis* spp., *Pyramimonas* spp. and *Chrysochromulina* spp. (Throndsen, 1969, 1976; Backe-Hansen and Throndsen, 2002a,b; Dahl and Johannessen, 1998). The quantitative data available are based on serial dilution cultures and most probable number estimates and are hence uncertain since the method is known to be both selective and to underestimate the *in situ* abundance (e.g. Throndsen, 1969, 1976; Backe-Hansen and Throndsen, 2002b).

Studies applying different molecular techniques to elucidate the picoplankton community composition corroborate observations based on cultures and light microscopy although the areas studied are not overlapping. By rRNA gene cloning and sequencing, Díez et al. (2001) found that prasinophytes were the most abundant and widespread algal group and that two Atlantic libraries contained clones related to *Micromonas pusilla*, *Emiliana huxleyi* and *Gymnodinium mikimotoi*. Using pigment analysis, molecular probes and flow cytometry to investigate the marine picoeukaryotic diversity in samples collected between the Norwegian, Greenland and Barents Seas, Not et al. (2005) found that *M. pusilla* was a dominant member of the picoeukaryotic community in both coastal and nutrient rich environments, whereas haptophytes seemed to be more important in open waters. There are also recent studies suggesting that the latter group is important in arctic seas (Not et al., 2005; Lui et al., 2009). Molecular studies have in addition revealed the presence of many novel taxa (Lovejoy et al., 2006).

Satellite ocean color data is a powerful tool to assess the abundance and spatial near surface distribution of phytoplankton in marine and coastal waters during cloud free conditions. This type of satellite data measures the spectral intensity of the light emerging from the ocean surface, which is related to the concentrations of color producing agents in the upper water masses, as well as the pure water itself. After correction of the remotely

sensed signal contribution from the atmosphere, such ocean color data are for oceanic (Case-1, e.g. Morel and Prieur, 1977) waters dominated by the abundance of the chl *a* pigment. For more optically complex coastal waters also dissolved organic compounds and suspended sediments influence the optical signal emerging from the water surface (e.g. Pozdnyakov et al., 2005; Folkestad et al., 2007; Korosov et al., 2009). Accordingly, the satellite ocean color data provide limited capabilities to discriminate between different algae genus and species, but provide information of the total chl *a* concentrations in the surface layer.

The co-occurrence of bacteria and viruses and the temporal and spatial variation of these planktonic groups in relation to phytoplankton have been addressed only in a few studies in Norwegian coastal waters. Bratbak et al. (1990) described a spring diatom bloom in Raunefjorden in western Norway and observed that the culmination of the diatom bloom was followed by a peak in the concentration of bacteria and an increase in the concentration of heterotrophic flagellates. The concentration of viruses varied through the spring bloom from  $5 \times 10^5$  in the prebloom situation to a maximum of  $1.3 \times 10^7$  viruses  $\text{mL}^{-1}$ . Following specific host-virus systems Bratbak et al. (1995) reported that the collapse of an *Emiliana huxleyi* bloom with a maximum cell density of ca.  $8 \times 10^3$  cells  $\text{mL}^{-1}$  was accompanied by a simultaneous increase in large virus-like particles (LVLP) reaching ca.  $1.8 \times 10^6$  LVLP  $\text{mL}^{-1}$ . The concentrations of *Synechococcus* and cyanophages have been found to co-vary through the year and with the highest concentrations in the autumn,  $7.3 \times 10^4$  *Synechococcus* cells  $\text{mL}^{-1}$  and  $7.2 \times 10^3$  cyanophage  $\text{mL}^{-1}$  (Sandaa and Larsen, 2006). Larsen et al. (2004) described succession and diversity of algae, bacteria and viruses in relation to environmental changes from February 15th to April 27th in Raunefjorden Western Norway and concluded that viroplankton are intimately linked to the rest of the microbial community and possibly act as an internal driving force in spring bloom successions.

The purpose of the present study was to explore the diversity and variation of the plankton community in Skagerrak and Norwegian coastal waters and to compare for the first time the data obtained by a variety of different methods including flow cytometry, light and epifluorescence microscopy, *in situ* chl *a* measurements and satellite remote sensing images of chl *a* (SeaWiFS).

## 2. Material and methods

### 2.1. Sampling

The samples were collected on May 5–7–2001 along three cruise transects from Jæren, Lista and Oksøy on the south coast of Norway and across the Norwegian Trench into the North Sea and Skagerrak (Fig. 1). The position and length of each leg were Leg #1 (Jæren) from 58°40'N, 5°27'E to 58°13'N, 4°07'E (50 nautical miles); Leg #2 (Lista) from 58°06'N, 6°32'E to 57°30'N, 6°0'E (41 nautical miles) and Leg #3 (Oksøy) from 58°01'N, 8°06'E to 57°25'N, 8°26'E (38 nautical miles). For each transect we sampled six stations at 7–10 nautical mile distance between 9 a.m. and 6 p.m. At each station we made one cast for CTD and *in situ* fluorescence measurements to locate the chl *a* maximum (the sampling depths requiring extra sample volume for parameters not included in this report) and then a separate cast for collecting water samples. The sampling depths were 0.5, 5, 10, 20, 50 and 200 m, and in addition the depth of the chl *a* maximum if not approximately coinciding with the fixed depths. In shallow waters (<200 m deep) the deepest sample was collected 10–70 m above the seafloor.

In addition to the three transects, we also followed a drifting buoy (Leg #4) for 55 h starting at 9 a.m. on May 8. The buoy had a

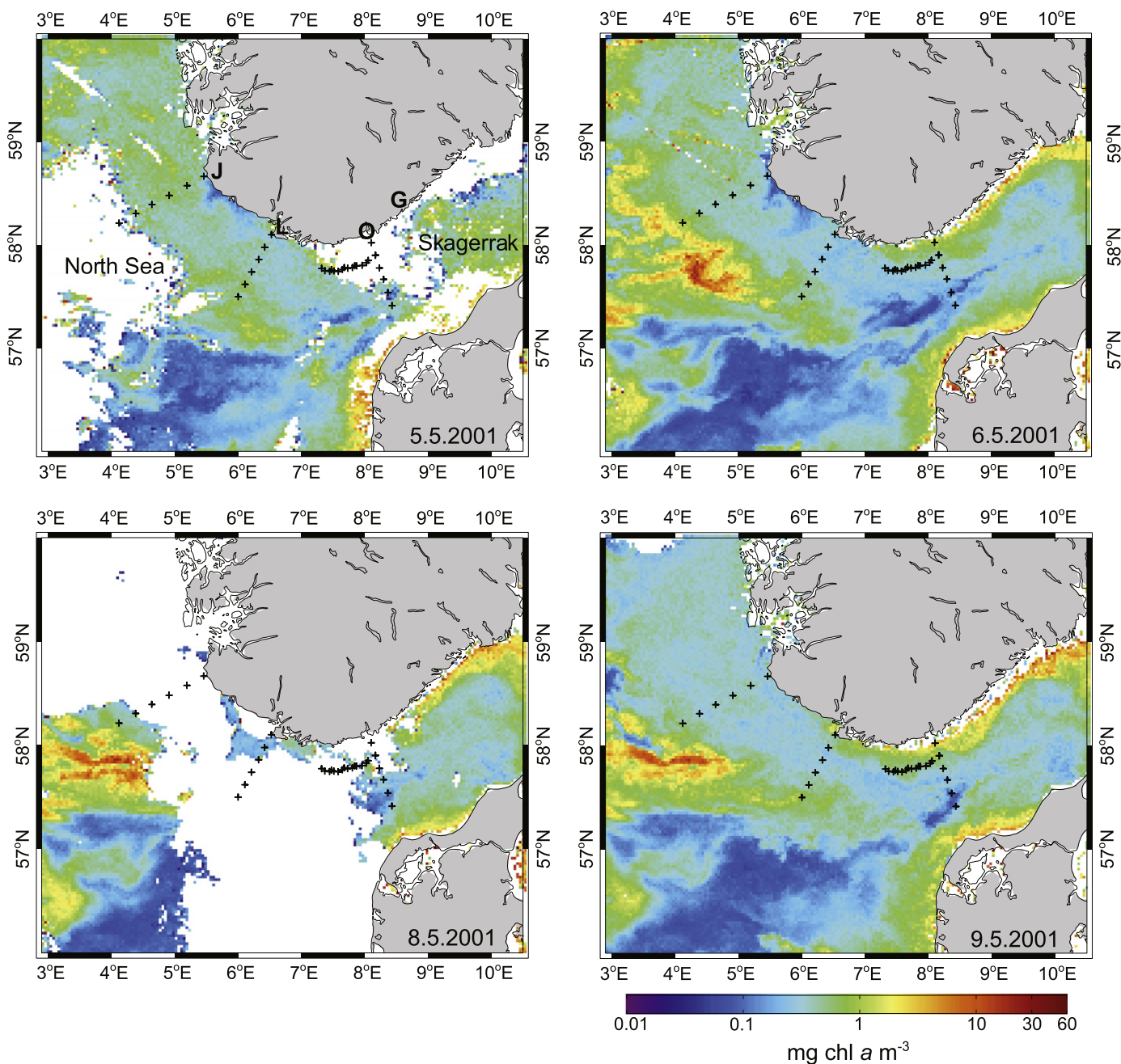


**Fig. 1.** Maps showing sampling stations superimposed on the satellite images (SeaWiFS) of the chl *a* distribution on the 5th, 6th, 8th and 9th of May 2001, respectively. The transects are from west to east Leg #1 (Jæren, sampled May 5th); Leg #2 (Lista, sampled May 6th); and Leg #3 (Oksøy, sampled May 7th). Leg 4 followed a drifting buoy along the coast from east to west (sampled May 8th–10th). The locations of Jæren, Lista, Oksøy and Grimstad are indicated by letters on the map of May 5th.

subsurface sail of ca. 20 m<sup>2</sup> at approximately 20 m depth, it was deployed at 57°54' N, 8°10'E on May 7, 22 p.m. and during sampling it drifted from 57°51' N, 8°03'E to 57°46' N, 7°19'E (24 nautical miles). Samples were collected close to the buoy every 4 h at 2, 10, 30, 50 and 200 m depth and at the chlorophyll maximum determined by *in situ* fluorescence (see below) which was between 15 and 25 m.

## 2.2. Flow cytometry sample processing and analysis

Analyses were performed with a FACSCalibur flow cytometer (Becton Dickinson) equipped with standard filter set-up and with an aircooled laser providing 15 mW at 488 nm. The phytoplankton were analyzed onboard using fresh samples at high flow

rate ( $\sim 70 \mu\text{l min}^{-1}$ ) with the addition of 1  $\mu\text{m}$  fluorescent beads (Molecular Probes Inc., Eugene, OR). Autotrophic groups, including the cyanobacteria *Synechococcus* spp and cryptophyte populations, were discriminated on the basis of their side scatter (right angle light scatter, RALS), chlorophyll and phycoerythrin fluorescence (Fig. 2A, B).

Bacterial and viral enumeration was performed on samples fixed with glutaraldehyde (0.5% final concentration) and frozen in liquid nitrogen and stored at  $-70^\circ\text{C}$  until analysis after a few weeks. The samples were thawed immediately before staining and analysis. The thawed viral samples were diluted 10- to 100-fold in TE buffer (Tris 10 mM, EDTA 1 mM, pH 8) and stained with SYBR Green I (Molecular Probes Inc., Eugene, OR) for 10 min at  $80^\circ\text{C}$  in the dark (Marie et al., 1999). The thawed bacterial

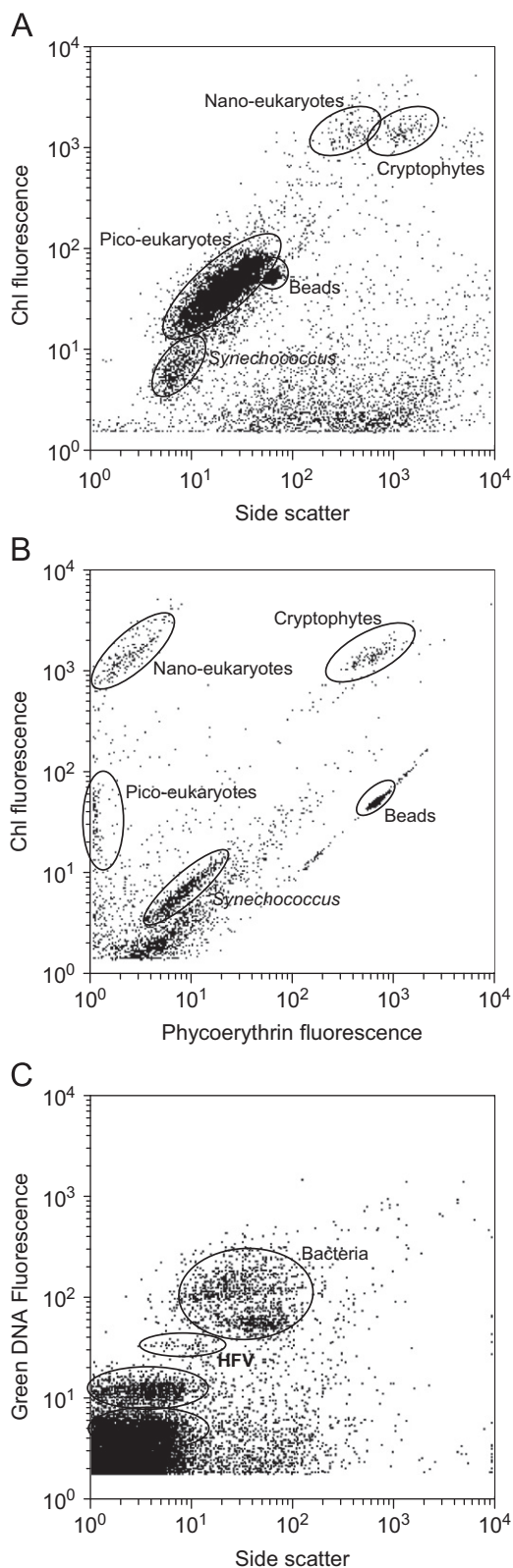


**Fig. 2.** Flow cytometry scatter plots showing how the different plankton communities and populations were defined. LFV, MFV and HFV are virus populations with low, medium and high fluorescence, respectively.

samples were also diluted 5- to 10-fold in TE buffer and stained with SYBR Green I for 15 min at room temperature in the dark. The final dilution of SYBR Green I was usually  $1 \times 10^{-4}$  of the commercial stock solution (Marie et al., 1999). However, when

the viral concentration was low we sometimes used  $0.5 \times 10^{-4}$  as this concentration then gave less signal noise in the viral samples while still high enough to stain all viral particles (Brussaard, 2004). Fluorescent microspheres (Molecular Probes Inc., Eugene, OR) with a diameter of  $0.95 \mu\text{m}$  were added to all samples as internal standard. The discriminator was set on the green fluorescence and the samples were analyzed for 1 min at a viral event rate between 100 and  $1000 \text{ s}^{-1}$ . Viruses were discriminated on the basis of their side scatter versus green DNA-dye fluorescence (Fig. 2C). Listmode files were analyzed using CYTOWIN (Vaulot, 1989; available at <http://www.sb-roscoff.fr/Phyto/index.php>) and WinMDI (Version 2.7, Trotter, available at <http://flowcyt.cyto.purdue.edu/flowcyt/software.htm>).

### 2.3. Microscopy

Phytoplankton and microzooplankton were identified by their morphology, size and autofluorescence, and enumerated by epifluorescence and inverted light microscopy. Fresh samples (2–10 mL) for determination of the trophic status of protists by epifluorescence microscopy were fixed with 3.6% glutaraldehyde, gently filtered onto black  $0.4 \mu\text{m}$  pore size nucleopore filters, stained with primulin and mounted on microscope slides in 10% glycerin (final concentrations) according to our own modification of the methods of Grebecki (1962), Hobbie et al. (1977) and Caron (1983). Samples for counting by inverted light microscopy were preserved with a glutaraldehyde–lugol mix (3.5% v/v) (Rousseau et al., 1990), stored at  $4^\circ\text{C}$  in the dark until further analysis, settled in 2, 10 or 50 mL sediment chambers, and counted and measured at  $200\times$ ,  $400\times$  and/or  $600\times$  magnification. Cell volume was calculated by approximation to the closest sample 3D shapes and converted into carbon biomass according to Menden-Deuer and Lessard (2000).

### 2.4. CTD and chlorophyll *a*

Temperature, salinity and *in situ* chl *a* fluorescence data were obtained with a SD204 CTD with a Sea Point fluorometer (SAIV A/S, Environmental Sensors and Systems, Bergen, Norway). Samples for chl *a* analysis were in addition filtered onto Whatman GF/F glassfiber filters and stored at  $-20^\circ\text{C}$ . The samples were analyzed within 2 weeks using a Turner Designs-10 fluorometer, 90% acetone extraction and acid corrections for phaeopigments (Strickland and Parsons, 1972).

### 2.5. Nutrients

Nitrate, phosphate and silicate concentrations were determined with a Skalar autoanalyzer at Institute of Marine Research (Bergen, Norway) following standard protocols (Strickland and Parsons, 1972; Rey et al., 2000). The samples were preserved with 1% (v/v) chloroform and stored in the dark at  $4^\circ\text{C}$  until analysis.

### 2.6. Satellite remote sensing

In May 2001, the US SeaWiFS ocean color sensor was in operation and cloud free conditions occurred in parts of the investigations areas during several days prior to, during and after our field investigations. The data used in this study was made available by the Nansen Center (<http://HAB.nerc.no>) in near real-time for use in planning of the field investigations. For this publication a re-processed using the NASA SEADAS OC4 (O'Reilly et al., 1999) software and global Case-1 water algorithms were used that is not taking into account the specific optical properties of the coastal Norwegian waters. For the application in

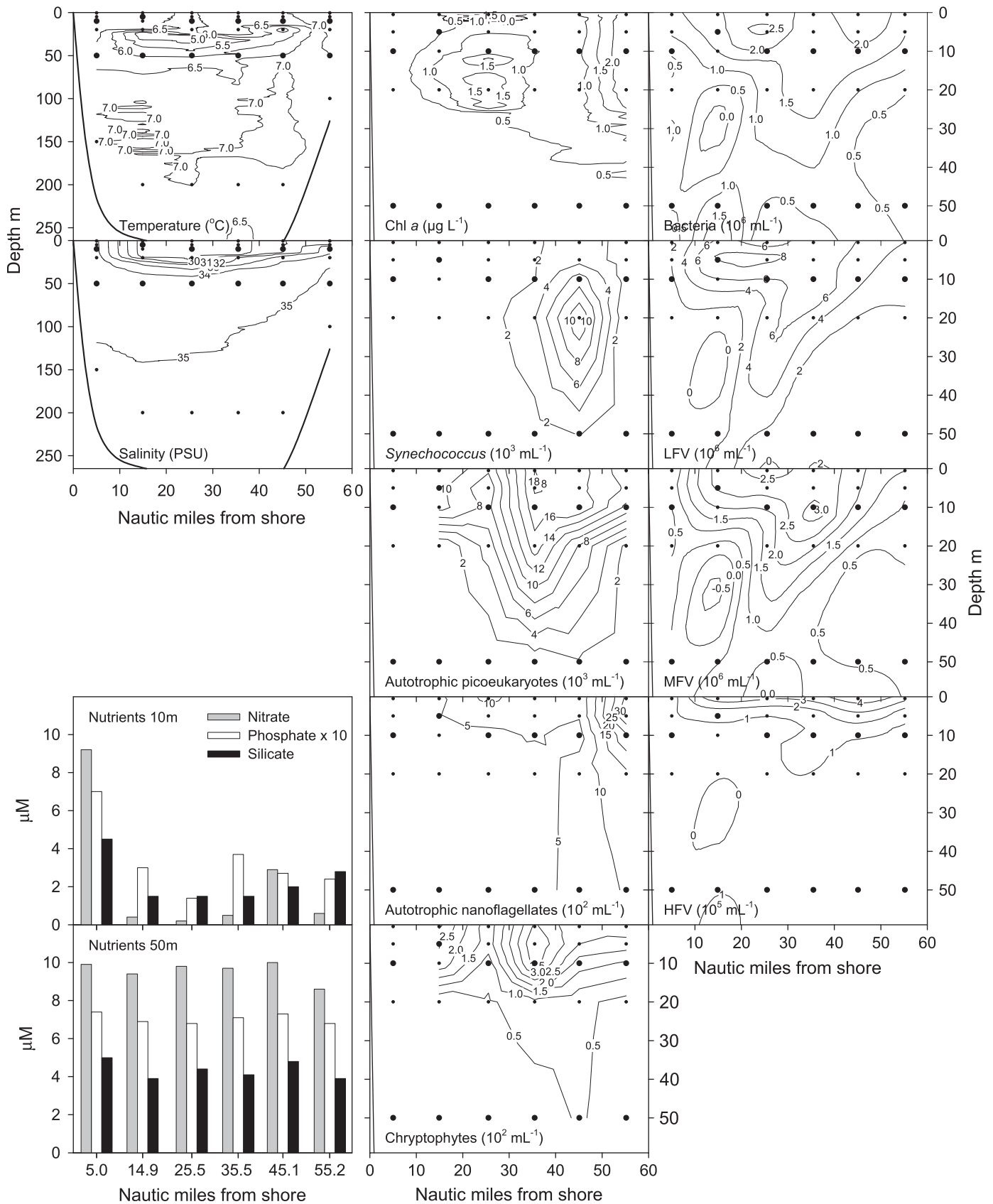


**Fig. 3.** Leg #1: Variations in temperature, salinity and nutrient concentrations; chlorophyll *a* concentration (based on *in situ* fluorescence) and flow cytometry counts of different phytoplankton, bacteria and viruses (cf. Fig. 2) from Jæren on the south coast of Norway and across the Norwegian trench into the North Sea. Position and depth of water samples are indicated by black dots in the isopleth plots, the larger dots indicate the samples examined by light microscopy.

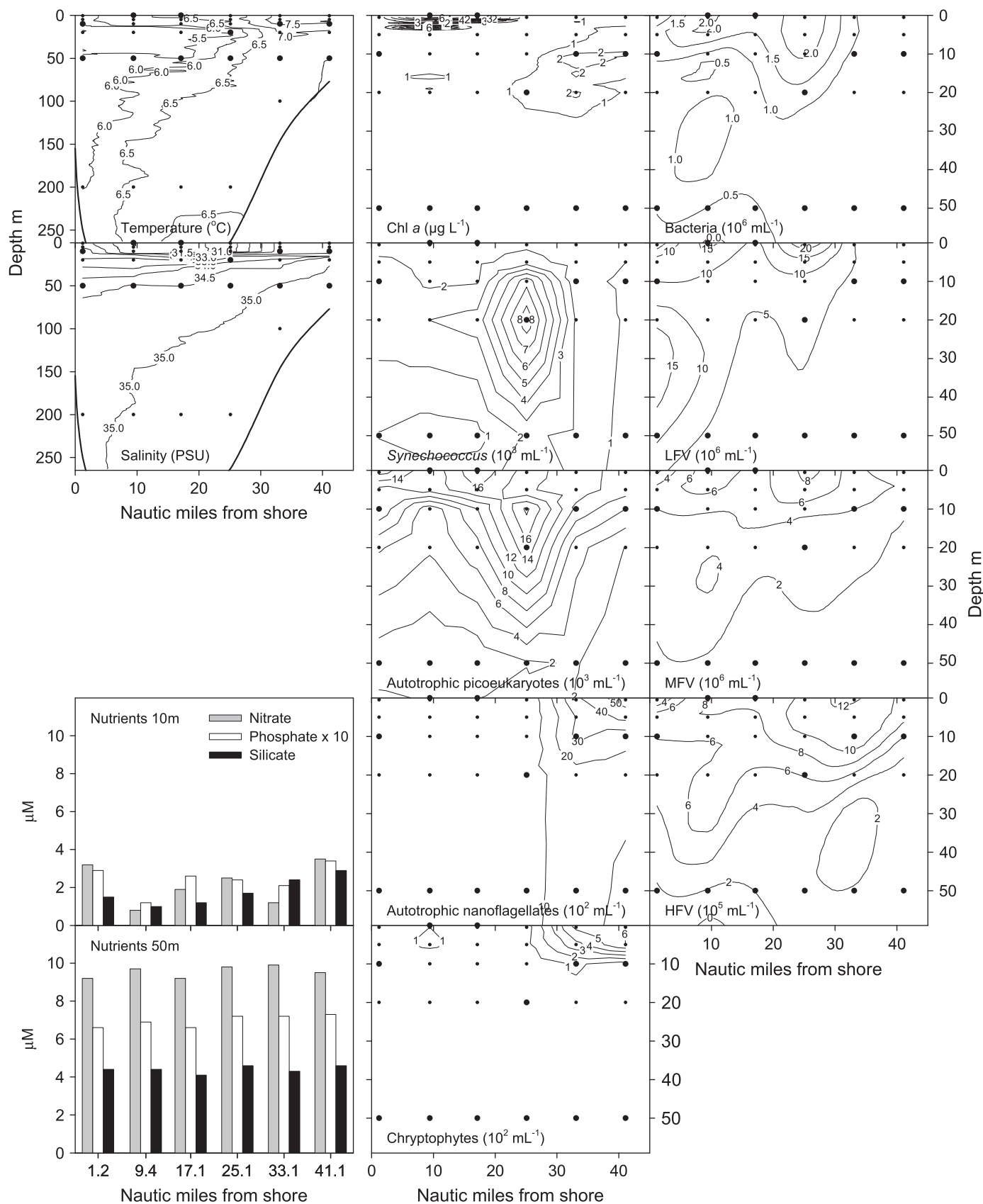


**Fig. 4.** Leg #2: Variations in temperature, salinity and nutrient concentrations; chlorophyll *a* concentration (based on *in situ* fluorescence) and flow cytometry counts of different phytoplankton, bacteria and viruses (cf. Fig. 2) from Lista on the south coast of Norway and across the Norwegian trench into the North Sea. Position and depth of water samples are indicated by black dots in the isopleth plots, the larger dots indicate the samples examined by light microscopy.

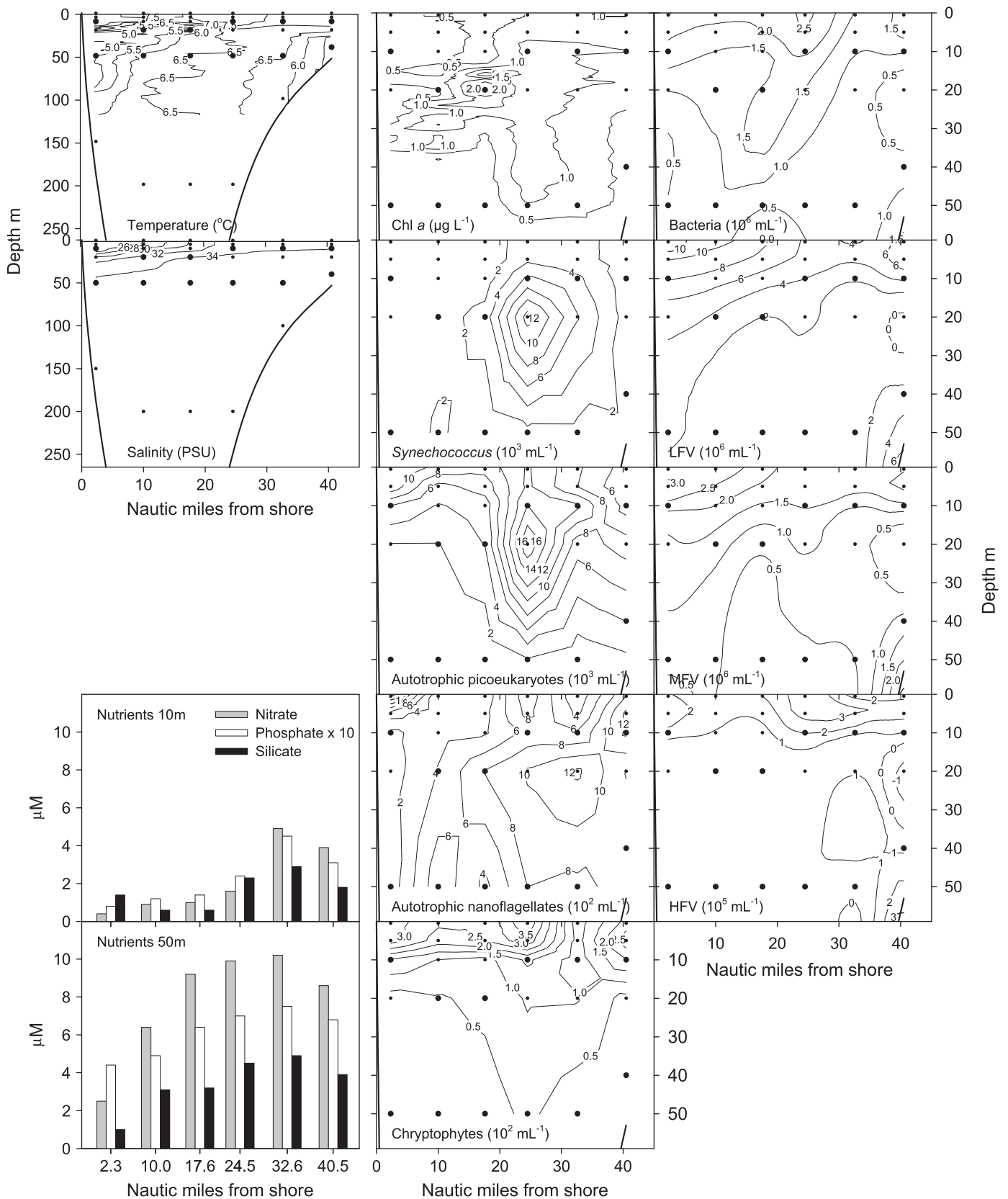


**Fig. 5.** Leg #3: Variations in temperature, salinity and nutrient concentrations; chlorophyll *a* concentration (based on *in situ* fluorescence) and flow cytometry counts of different phytoplankton, bacteria and viruses (cf. Fig. 2) from Oksøy on the south coast of Norway and across the Norwegian trench into Skagerrak. Position and depth of water samples are indicated by black dots in the isopleth plots, the larger dots indicate the samples examined by light microscopy.

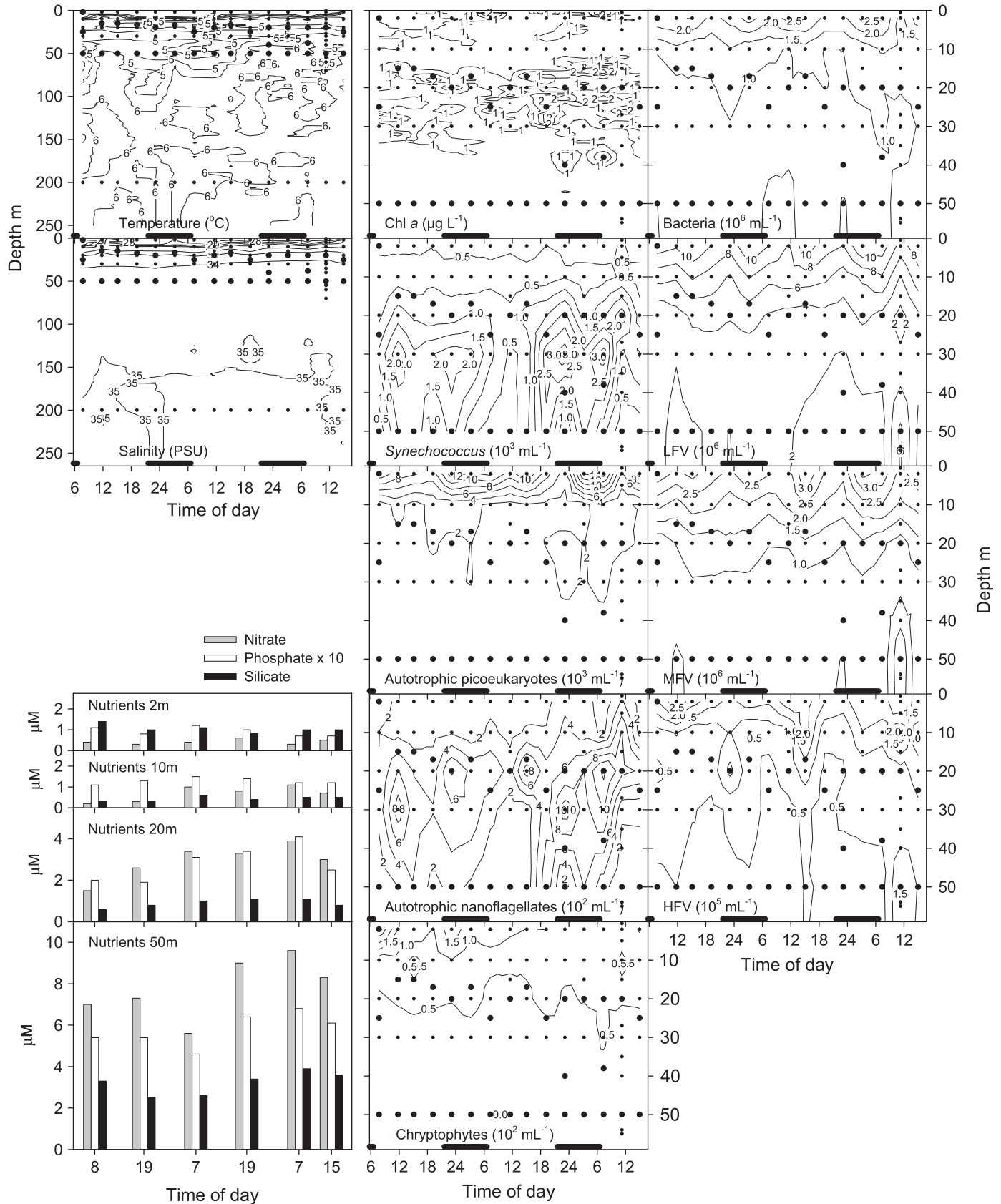


**Fig. 6.** Leg #4: Variations in temperature, salinity and nutrient concentrations; chlorophyll *a* concentration (based on *in situ* fluorescence) and flow cytometry counts of different phytoplankton, bacteria and viruses (cf. Fig. 2) during 55 h following a drifting buoy in Skagerrak. Position and depth of water samples are indicated by black dots in the isopleth plots, the larger dots indicate the samples examined by light microscopy. Black bar at the x-axis indicates dark period (sunset to sunrise).



this study the expected quality of the derived chl *a* concentrations based on this global algorithm was considered to be sufficient.

### 2.7. Statistical analysis

The quantitative biological data, including the chl *a* measurements (i.e. *in situ* fluorescence) and the population abundances obtained by flow cytometry, were examined using Statistica 8.0 (StatSoft, Tulsa, OK, USA). For this statistical analysis, we replaced all data by their logarithms and normalized each variable to have 0 mean and standard deviation (SD) of 1. Statistical analysis concerning distribution of species was based on untransformed microscopy counts.

## 3. Results and discussion

### 3.1. Hydrography

The data on hydrography (temperature and salinity), nutrients (N, P, Si), chl *a* and abundance of organisms and viruses are shown for each transect in Figs. 3–5. The salinity showed a strong stratification of the water column with the relatively fresh (< 30–34‰) coastal current broadening and deepening as the water flows out of Skagerrak (Leg #3) and reaches Jæren on the Norwegian west coast (Leg #1). In the deep Norwegian Trench, Atlantic water (> 35‰) penetrates across the Lista transect (Leg #2) but not as far into Skagerrak as the Oksøy transect (Leg #3) where the deep water masses were less saline. The temperature ranged from 5 to 7 °C and followed the variation in salinity. The pattern was consistent with the surface extension of the higher chl *a* concentrations observed in the satellite images (see Fig. 1, not all available and analyzed images are included in the paper). Between May 1st and 11th, the front location of the high chl *a* concentrations was advected from along the coast from around Grimstad to Lista (Fig. 1) during about 10 days, which is equivalent of a speed of about 0.33 knots (compared with the drift velocity of the buoy estimated to 0.4 knots).

### 3.2. Nutrients

The nutrient concentrations at the surface (i.e. 10 m) were typically lower ( $2 \pm 2 \mu\text{M}$  nitrate,  $0.2 \pm 0.1 \mu\text{M}$  phosphate and  $2 \pm 1 \mu\text{M}$  silicate (mean  $\pm$  SD)) than at 50 m depth ( $9 \pm 2 \mu\text{M}$  nitrate,  $0.7 \pm 0.1 \mu\text{M}$  phosphate and  $3.9 \pm 0.9 \mu\text{M}$  silicate). At 50 m depth, the nutrient concentrations did not vary much along Leg #1 and 2, while across Skagerrak at Leg #3 the values tended to be lower both on the Norwegian and on the Danish side. At the surface, elevated nutrient values were found close to the Norwegian coast on Leg #1 and towards the Danish coast on Leg #3.

### 3.3. Chlorophyll

Data from the three first legs (sampled on May 5th, 6th and 7th 2001, respectively) were compared with a SeaWiFS image taken on May 6th 2001 (Fig. 1). For the fourth leg, a SeaWiFS image taken on May 9th 2001 was used.

*In situ* chlorophyll and remotely derived values compared quite well for the two first legs (Fig. 7A, B) using the standard OC4 chl *a* product. The relatively high *in situ* chlorophyll fluorescence observed at the surface 10–20 nautical miles offshore in Leg #2 (Figs. 4 and 7) was, however, not confirmed by chl *a* measurements and was not obviously apparent on the satellite images (Fig. 1). This discrepancy might be explained by small scale patchiness since the *in situ* fluorescence measurements and the sampling of water for chl *a* analysis were made on separate

casts and the *in situ* fluorescence indeed appeared to be very patchy close (0–4 m depth) to the surface (Fig. 4; Supplementary Fig. 1). On the third leg (Fig. 7C), we observed good coincidence of *in situ* and remote sensing data only in open waters (30–40 nautical miles offshore) while closer to the shore (2–25 nautical

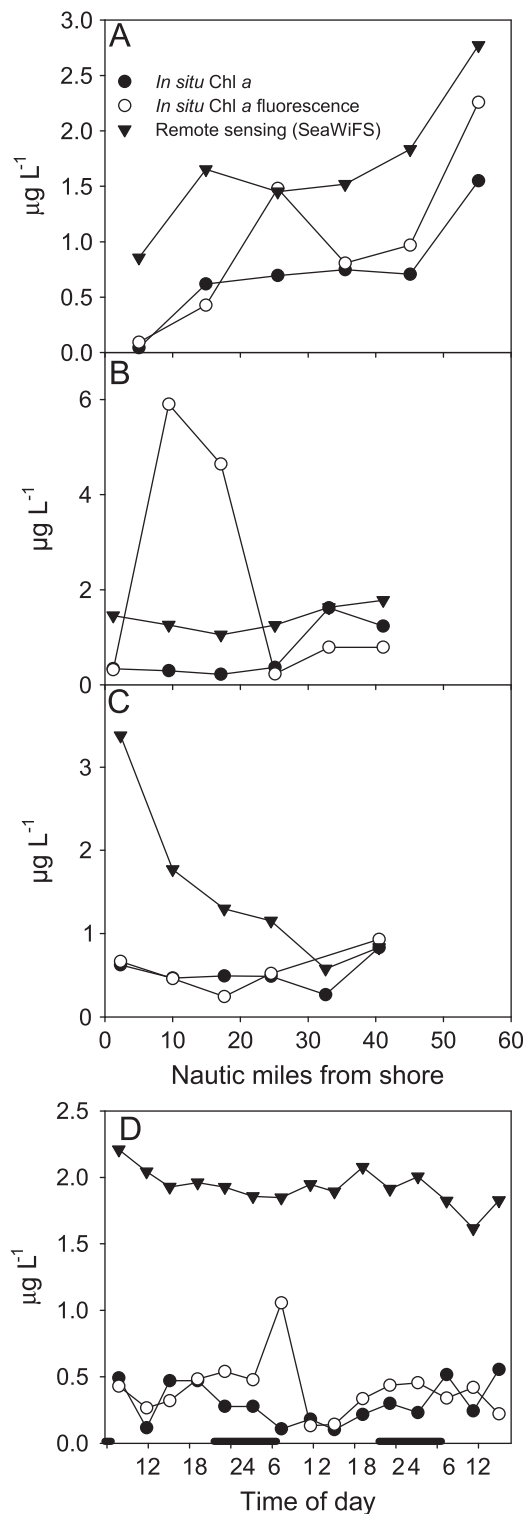


**Fig. 7.** Comparison of *in situ* surface and remote sensing chlorophyll *a* values along Leg #1 (A), Leg #2 (B), Leg #3 (C) and Leg #4 (D), respectively. *In situ* values are from both chl *a* collected on filters (sampling depth 0.5 m) and from *in situ* chl *a* fluorescence (average of values recorded between 0 and 1 m); remote sensing data are based on SeaWiFS images. Time differences between observations may be more than 30 h and is not compensated for in the analysis.

miles offshore), where the measurements may be expected to be more influenced by sediments and dissolved organic matter of terrestrial origin, remote sensing chl *a* was overestimated compared to the *in situ* data. The same factors might explain the difference between remote sensing and *in situ* values in Leg #4 (Fig. 7D) for which sampling was about 10 nautical miles offshore.

The accuracy of OC4 algorithm was in general found to be rather high, but with some bias in the exact values of the chl *a* estimates. A similar analysis was made using the *in situ* observations and satellite data from May 1st, 2nd and 11th. Due to longer time discrepancy between these pair of observations the correlation between them was also found to be poorer.

#### 3.4. Phytoplanktonic groups (FCM) and identification of species (EFM, LM)

The distribution of *Synechococcus* along the three transects was remarkably similar and the same was true for the autotrophic picoeukaryotic community (Figs. 3, 4 and 5). Relatively high abundance, up to  $1.3 \times 10^4$  cells mL<sup>-1</sup>, of *Synechococcus* was found at 20 m depth 25–45 nautical miles from shore on Leg #1–3 and this localized bloom appeared to stretch out for more than 100 nautical miles from Skagerrak and up the south west coast of Norway. The abundance of autotrophic picoeukaryotes, which reached a maximum of  $1.8 \times 10^4$  cells mL<sup>-1</sup>, had a distribution that was similar to the *Synechococcus* (cf. Table 1) but with higher concentration near the surface. The distributions of autotrophic nanoflagellates (maximum abundance  $5.7 \times 10^3$  cells mL<sup>-1</sup>) and chryptophytes (maximum abundance  $6.0 \times 10^2$  cells mL<sup>-1</sup>) were also comparable along the three transects (Figs. 3–5) with generally higher abundances at the offshore stations and at the surface above 10 m depth. The inventory of these communities is listed in Supplementary Table 1 and discussed below. The sampling of the transects ranged over a period of about 10 h and the apparent spatial distribution may to some extent also be interpreted as a consequence of a diel variation (see Section 3.6).

The abundances of *Synechococcus*, autotrophic picoeukaryotes and nanoflagellates observed in this study were in the same range or higher than those observed during a spring bloom in these waters ( $0.3\text{--}3 \times 10^3$  *Synechococcus* mL<sup>-1</sup>,  $0.06\text{--}1.4 \times 10^4$  picoeukaryotes mL<sup>-1</sup> and  $0.6\text{--}7.1 \times 10^3$  nanoflagellates mL<sup>-1</sup>) (Larsen et al., 2004). However, they were in the same range or lower than during a summer bloom ( $3.5 \times 10^4$  *Synechococcus* mL<sup>-1</sup> and  $2.0 \times 10^4$  picoeukaryotes mL<sup>-1</sup>) (Sandaa and Larsen, 2006). The

abundances of *Synechococcus* and of autotrophic picoeukaryotes in Norwegian coastal waters appear in general to be lower than in upwelling regions where peak abundances are reported to  $2\text{--}150 \times 10^4$  *Synechococcus* mL<sup>-1</sup> (typical range  $10^3\text{--}10^5$  mL<sup>-1</sup>) and  $0.4\text{--}8.6 \times 10^4$  picoeukaryotes mL<sup>-1</sup> (typical range  $10^3\text{--}10^4$  mL<sup>-1</sup>, termed “small photosynthetic eukaryotes” in this study) (Sherr et al., 2005 and references therein). The values are, however, in the same range ( $0.5\text{--}50 \times 10^3$  cells mL<sup>-1</sup>) as those observed in the upper euphotic layer of the subarctic Pacific Ocean, the northern Gulf of Alaska and the Bering Sea (Liu et al., 2002; Zhang et al., 2008).

The distribution of the different phytoplankton groups may be interpreted to suggest that the nanoflagellates and chryptophytes found closer to the surface require more light and lower nutrient concentrations than *Synechococcus* and the picoeukaryotes found at and below the halocline where there is less light and higher nutrient concentrations. The halocline (and hence pycnocline) characteristic of the coastal current is deepening towards land (Figs. 3–5) and this may prevent *Synechococcus* and the autotrophic picoeukaryotes to move further onshore as light may be limiting at the depth of the halocline where sufficiently high nutrient concentrations are found. These results seem contradict the notion that smaller forms (i.e. *Synechococcus* and picoeukaryotes in this context) are predominating in environments characterized by low nutrient concentrations compared to larger forms (i.e. nanoflagellates and chryptophytes in this context) (Bell and Kalf, 2001 and references therein). However, in the dynamic coastal ecosystem considered here, where the physiochemical environment is complex and highly variable and where nutrients may be low but not permanently depleted, we should not expect the community composition and population distribution to parallel large scale variations observed along oligotrophic–eutrophic and oceanic–coastal gradients.

#### 3.5. Bacteria and viruses

The abundance of bacteria in surface water between 0 and 20 m was typically  $10^6$  cells mL<sup>-1</sup>, while below 20 m the abundance was in general lower than  $10^6$  cells mL<sup>-1</sup>. The highest values were found 25–35 nautical miles offshore with  $2\text{--}2.5 \times 10^6$  cells mL<sup>-1</sup> (Figs. 3–5). The abundance of Low Fluorescent Viruses (LFVs) and Medium Fluorescent Viruses (MFVs) (Fig. 2C) ranged from  $1\text{--}20 \times 10^6$  and  $0.5\text{--}8 \times 10^6$  virus mL<sup>-1</sup>, respectively. The highest values were found in the surface waters and the distribution

**Table 1**  
Partial correlation controlling for depth between the biological parameters (chl *a* (i.e. *in situ* fluorescence) and population abundances obtained by flow cytometry). The original data were replaced by their logarithms and each variable normalized to have 0 mean and SD of 1.

	Chl <i>a</i>	<i>Synechococcus</i>	Autotrophic picoeukaryotes	Chryptophytes	Autotrophic nanoflagellates	Bacteria	Low Fluorescence Virus	Medium Fluorescence Virus
<i>Synechococcus</i>	0.374***							
Autotrophic picoplankton	0.537***	0.677***						
Chryptophytes	0.471***	0.340***	0.662***					
Autotrophic nanoflagellates	0.597***	0.492***	0.506***	0.619***				
Bacteria	0.077	0.224**	0.432***	0.372***	−0.067			
Low Fluorescence Virus	−0.148	−0.059	0.247**	0.097	−0.363***	0.496***		
Medium Fluorescence Virus	0.068	0.194*	0.484***	0.163*	−0.017	0.256**	0.685***	
High Fluorescence Virus	0.145	0.372***	0.385***	0.085	0.212**	0.037	0.242**	0.753***

\*  $p < 0.05$ .

\*\*  $p < 0.01$ .

\*\*\*  $p < 0.001$ .

followed to a large extent that of the bacteria. The highest abundance of the High Fluorescent Viruses (HFVs) (Fig. 2C) was found above 10–20 m depth with  $1\text{--}10 \times 10^5$  VLP mL<sup>-1</sup>. The correlations between the different virus groups and possible hosts are considered in Section 3.8. As for the phytoplankton, the apparent spatial distribution of bacteria and viruses may in part also be interpreted to be a consequence of a diel variation (see Section 3.6.).

Assuming the LFVs to be dominated by and representative for bacteriophage abundance (cf. Larsen et al., 2004 and references therein), the overall virus:host ratio for bacteria was found to be  $4.3 \pm 2.4$  (mean  $\pm$  SD). The ratio was higher near the coast (< 20 nautical miles) than at offshore stations (> 20 nautical miles), i.e.  $4.6 \pm 2.5$  and  $3.4 \pm 1.6$ , respectively (mean  $\pm$  SD,  $p < 0.004$ , DF = 148). However there was no significant difference ( $p < 0.09$ ) when comparing surface (< 20 m) and deep water (> 20 m) samples. These virus:host ratios were in any case in the low range of values reported in the literature (see Weinbauer, 2004).

### 3.6. Lagrangian sampling and diel variation (leg #4)

In Leg #4 we intended to follow the same water mass over time using a drifting buoy with a subsurface sail at ca. 20 m depth. The temperature and salinity we measured at 20 m over the 55 h period did not show significant variations compared to the changes observed above and below this depth (Fig. 6). This suggests that we managed to follow the same water mass at 20 m depth and that the water masses above and below were moving at different speed or in different direction. This conclusion was not immediately supported by the nutrient data (Fig. 6). The nutrient concentration changed at all depth, including at 20 m, and it may thus be questioned how much of this change was due to *in situ* biological and physical processes and how much it was also due to sampling of different water masses.

Most parameters, including chlorophyll, phytoplankton, bacteria and viruses showed no sizeable variation at 20 m depth. The exceptions were the autotrophic nanoflagellates and the high fluorescent viruses. The abundance of autotrophic nanoflagellates and *Synechococcus* showed some variations below 20 m depth, which may be interpreted as change in water mass with a corresponding change in population density. The most intriguing variation was the apparent diel variation in autotrophic picoplankton, bacteria and all virus types; and to some extent also in chl *a*; in the surface waters. The values were in general higher around noon and late at night and lower in the evening (Fig. 6; Supplementary Fig. 2). This diel variation agrees with the results from the transects showing that the highest abundances of bacteria, virus and autotrophic picoeukaryotes were found 25–35 nautical miles offshore at stations sampled between 13.00 and 14.00 local time. The variation along the transects was, however, larger (mean  $\pm$  SD of normalized surface abundances =  $1 \pm 0.9$ ) than during the Lagrangian study ( $1 \pm 0.2$ ) suggesting that the spatial distribution was not only a consequence of diel variation.

Diel variations in microbial parameters have been observed several times, and viral production and abundance are often found to coincide or succeed periods of high bacterial activity (Heldal and Bratbak, 1991; Jiang and Paul, 1994; Weinbauer et al., 1995; Winter et al., 2004). Light is the most obvious driving force for diel variations in natural ecosystems, but the link seems to be complex since we observed two maxima and two minima per 24 h. The processes possibly modulating the diel variation include grazing (Dolan and Simek, 1999), viral decay (Jacquet et al., 2002) and photoinhibition (Vaulot and Marie, 1999). The diel variations found in phytoplankton abundances and *in situ* chl *a* fluorescence have obvious implications for both the validation and applications of the satellite derived information, since the optimal and used

satellite passes at our latitude were confined daily to be around 11 a.m. mean local solar time.

### 3.7. Microscopic counts, biomass and species

The biomass contribution of the dominating species (in terms of average biomass of all samples) and of the different plankton size groups in different water masses as determined by light

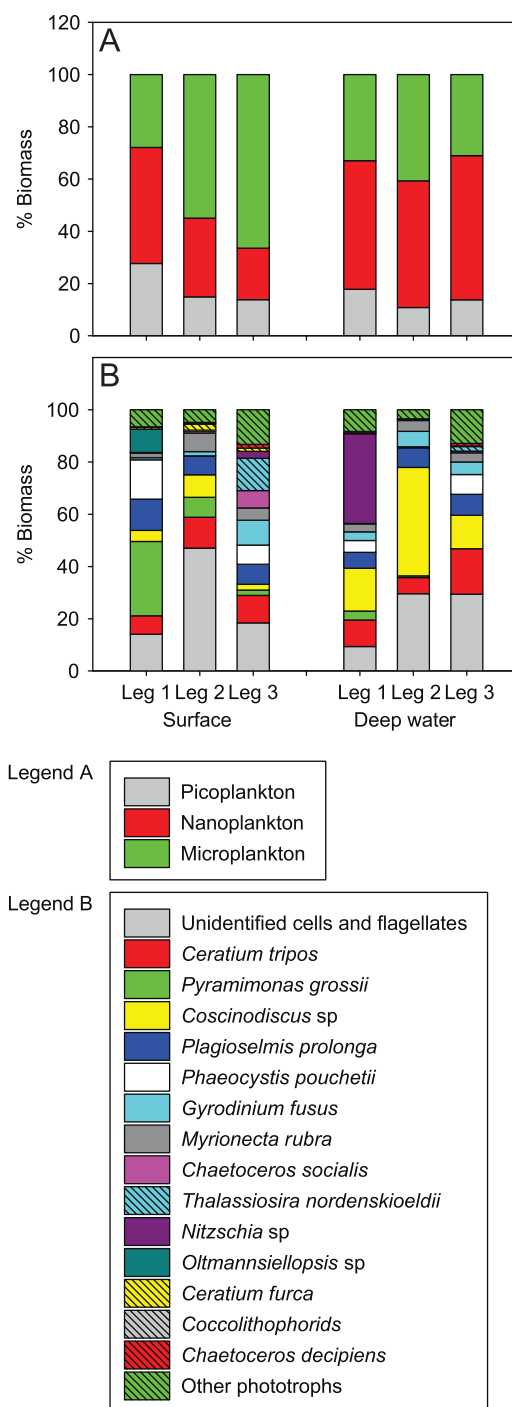


**Fig. 8.** Biomass contribution of the different phytoplankton size groups (A) and of the dominating phytoplankton species (B) in the three transects. Surface samples were collected at 5 m depth and deep water samples at 50 m. The species considered dominating are dominating in terms of their average biomass (average of all samples) and they comprise together about 90% of the biomass. A single observation of a few very large *Halosphaera viridis* cysts is excluded from the Leg 2 data.

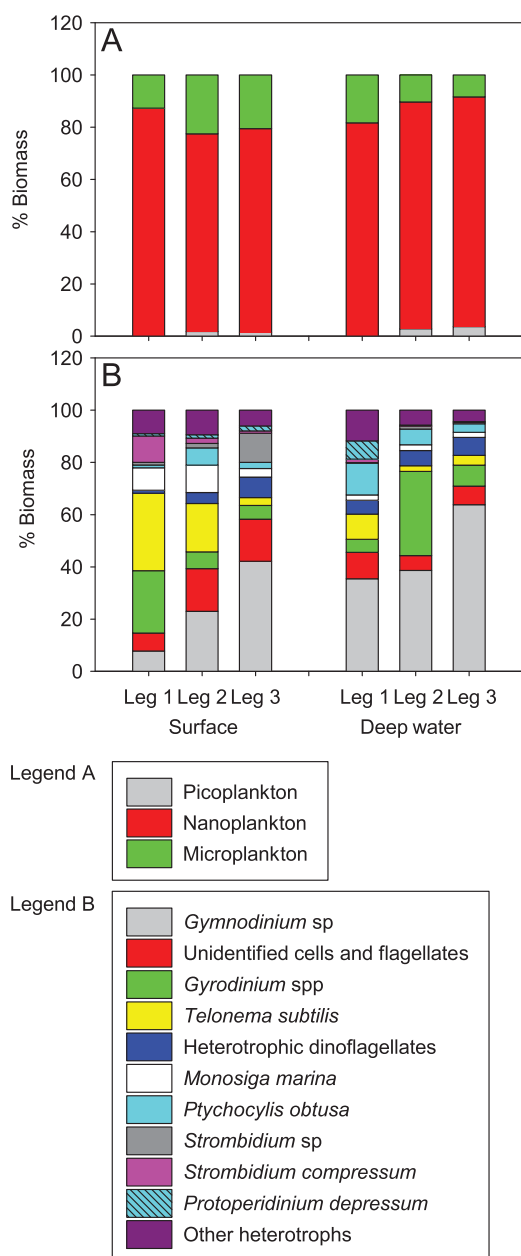


**Fig. 9.** Biomass contribution of the different heterotrophic plankton size groups (A) and of the dominating heterotroph species (B) in the three transects. Surface samples were collected at 5 m depth and deep water samples at 50 m. The species considered dominating are dominating in terms of their average biomass (average of all samples) and they comprise together about 90% of the biomass.

microscopy is summarized in Figs. 8 and 9. All plankton species identified, their occurrence, abundance and biomass are listed in Supplementary Tables 1 and 2. In the phototrophic community, microplankton made on the average up to  $4 \pm 7\%$  (mean  $\pm$  SD) of the abundance and  $49 \pm 26\%$  of the biomass while the picoplankton made up ca.  $70 \pm 28\%$  of the abundance and  $17 \pm 14\%$  of the biomass. Heterotrophic micro- and nano-plankton made up  $29 \pm 17\%$  and  $70 \pm 18\%$  of the heterotrophic biomass, respectively, while in terms of abundance, the microplankton made up only  $2 \pm 4\%$ , the nanoplankton  $71 \pm 21\%$  and the picoplankton  $28 \pm 21\%$  of the community.

The abundance ( $97 \pm 8\%$ , mean  $\pm$  SD) and biomass ( $85 \pm 19\%$ ) of nanoplankton sized phototrophs was dominated by *Pyramimonas grossii*, *Phaeocystis pouchetii* (motile stage) and *Plagioselmis prolunga*, and by unidentified phototrophic cells. The microplankton

community was in terms of abundance dominated ( $71 \pm 32\%$ ) by *Chaetoceros socialis*, *Phaeocystis pouchetii* (colonial), *Thalassiosira nordenskiöldii*, *Gyrodinium fusus* and *Myrionecta rubra* but these forms made up only  $49 \pm 31\%$  of the biomass. Occasional occurrence of the larger *Coscinodiscus* sp., *Ceratium tripos* and *Halosphaera viridis* cysts made up additional  $33 \pm 32\%$  of the biomass.

The abundance ( $97 \pm 12\%$ ) and biomass ( $92 \pm 13\%$ ) of nano-plankton sized heterotrophs was both dominated by *Monosiga marina*, *Telonema subtilis*, *Gyrodinium* spp and *Gymnodinium* spp, and by unidentified heterotrophic cells. The heterotrophic micro-plankton community was in terms of abundance dominated ( $75 \pm 18\%$ ) by *Gyrodinium* spp, *Strombidium elegans*, *Strombidium compressum*, *Gymnodinium* sp, *Amphidinium sphaenoides* and by unidentified heterotrophic cells including dinoflagellates. These forms made up  $61 \pm 22\%$  of the heterotrophic microplankton biomass.

Along the transects there was a significant variation in distribution and abundance of different planktonic forms with *Synechococcus* and autotrophic picoeukaryotes as the most notable examples discussed above (Figs. 3–5). In surface waters the abundance of *Pyramimonas* cf. *grossii* and *Telonema subtilis* increased in abundance with increasing distance offshore ( $R=0.495$ ,  $p=0.037$  and  $R=0.601$ ,  $p=0.008$ , respectively) while the abundance of *Chaetoceros decipiens*, *Torodinium robustum* and *Myrionecta rubra* showed the opposite distribution ( $R=-0.52$ ,  $p=0.027$ ,  $R=-0.54$ ,  $p=0.021$  and  $R=-0.614$ ,  $p=0.007$ , respectively) with the highest concentration at the innermost stations. In deep water samples the group counted as “unidentified cells and flagellates” increased while *Myrionecta rubra* and *Amphidinium sphaenoides* decreased in abundance with increasing distance offshore ( $R=0.637$ ,  $p=0.005$ ,  $R=-0.485$ ,  $p=0.041$  and  $R=-0.493$ ,  $p=0.038$ , respectively). Grouping populations together according to size, phototrophy/heterotrophy and taxonomic affiliation did not disclose additional significant distribution patterns.

The plankton biomass composition in surface waters did also change to be more dominated by smaller forms as the water flows westward from Skagerrak and into the North Sea (Figs. 1, 8A and 9A). For the heterotrophic plankton this change was due to a decrease in the biomass of larger dinoflagellates and different unidentified forms, and an increase in biomass of the smaller *Gyrodinium* spp and *Telonema subtilis* (Fig. 9B). For the phytoplankton, however, the trend could not be accounted for by a successive change in community composition (Fig. 8B).

Studying the spatial distribution of phytoplankton along a 137 nautical mile transect in the eastern part of the North Sea, Škaloud et al. (2006) identified a total of 144 different algae including 85 species of diatoms and 44 species of dinoflagellates of which 25 were heterotrophic forms. In comparison, we identified 59 phototrophic and 45 heterotrophic plankton forms comprising 33 diatoms and 32 dinoflagellates including 19 heterotrophic forms. Only 27 algal species were common to both studies while the remainder was exclusive to one or the other. One reason we identified fewer species is that use of electron microscopy enabled Škaloud et al. (2006) to resolve species rich genera like *Navicula*, *Nitzschia*, *Thalassiosira* and *Protoperidinium* to the species level. Another reason may be that 51 of the species they identified were not found less than ca. 50 nautical miles offshore (i.e. on the three innermost stations) which is beyond our outermost stations, suggesting that their material included oceanic forms we did not sample here. However, we found 11 of these 51 species in our coastal samples implying that the coastal-oceanic distribution is not unambiguous.

The carbon-to-chlorophyll ratio was estimated to  $21 \pm 14$   $\mu\text{gC}/\mu\text{g chl } a$  (chl *a* measured on filters). This ratio is in the low end of most published values (e.g. Banse, 1977; Geider et al. 1997;

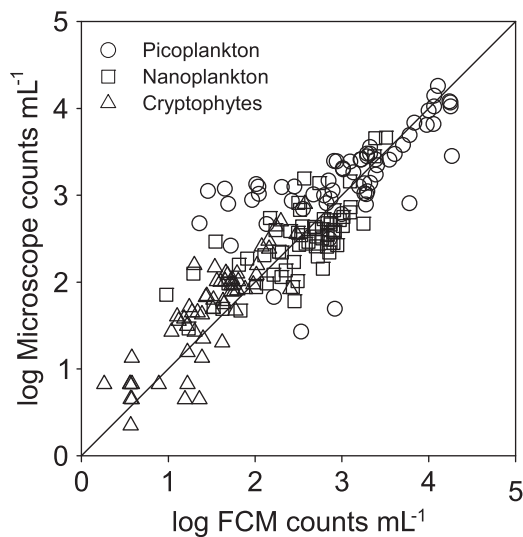


**Fig. 10.** Comparison of flow cytometry counts and microscopy counts of different phytoplankton communities. The line shows the 1:1 ratio. Log linear Type II regression gave the following equations (values below detection limit and zero values were omitted): Picoplankton:  $0.722X + 1.001$  ( $R=0.668$ ,  $p=2.27 \times 10^{-9}$ ,  $N=63$ ), Nanoplankton:  $0.826X + 0.387$  ( $R=0.741$ ,  $p=7.35 \times 10^{-13}$ ,  $N=67$ ), Cryptophytes:  $1.117X - 0.021$  ( $R=0.867$ ,  $p=1.66 \times 10^{-19}$ ,  $N=61$ ). All:  $0.911X - 0.305$  ( $R=0.875$ ,  $p < 1.0 \times 10^{-19}$ ,  $N=191$ ).

Sathyendranath et al., 2009 and references therein) also when considering that different phytoplankton forms have different C:chl *a* ratios and that the composition of the phytoplankton community, in terms of carbon biomass, was dominated by different flagellated forms ( $53 \pm 26\%$  mean  $\pm$  SD) together with diatoms ( $27 \pm 25\%$ ) and dinoflagellates ( $20 \pm 17\%$ ). However, with the over two orders of magnitude range in carbon-to-chlorophyll ratios reported in the literature (Veldhuis and Kraay, 2004) and the accuracy and precision of our biomass estimates, which were based on microscope sizing and volume to carbon conversion in mind, we are inclined to conclude that the agreement is good and that our biomass estimates are confirmed by the chl *a* measurements. It is moreover noteworthy that there was a reasonably good agreement between FCM counts and microscopy counts of different phytoplankton communities (Fig. 10). Together this suggests that the different procedures used (fixation, freezing, storage time, etc.) for the two counting techniques, and our interpretation of the FCM scatter plots (Fig. 2) did not introduce large systematic errors.

### 3.8. Statistical analysis

There were significant ( $p < 0.001$ ) positive correlations between all biological parameters (chl *a* (i.e. *in situ* fluorescence) and population abundances obtained by flow cytometry), except between chl *a* and LFV (data not shown). This is in accordance with many earlier studies (for review see Gasol and Duarte, 2000; Wommack and Colwell, 2000; Li et al., 2004) and presumably reflects that most planktonic groups co-vary with depth and with eutrophic compared to oligotrophic conditions.

When controlling the correlation for depth, the statistical analysis becomes more meaningful and showed that chlorophyll and the different phytoplankton groups were all positively correlated (Table 1). Bacterial abundance was, however, not correlated with chlorophyll but with three of the phytoplankton groups and with the low and medium fluorescent viral populations. There was no correlation between virus and chlorophyll and a variable correlation between viruses and the different phytoplankton groups. The only significant negative correlation was between the autotrophic

nanoflagellates and the low fluorescent viruses (Table 1). The lack of correlation between chlorophyll concentration and abundance of bacteria and of virus opposes many earlier observations (for review see Bird and Kalff, 1984; Maranger and Bird, 1995).

*Synechococcus* was positively correlated to the high and medium fluorescent viral populations (Table 1), apparently corroborating many earlier studies based on plaque assay or quantitative PCR reporting that high host and virus concentrations are co-occurring (e.g. Waterbury and Valois, 1993; Suttle and Chan, 1994; Mühling et al., 2005; Sandaa and Larsen, 2006). Based on experience (Sandaa and Larsen, 2006) we should expect to find cyanophages in the medium or low fluorescent virus populations but the latter was not correlated to *Synechococcus* (Table 1).

The correlations between the biological parameters and the nutrient concentrations, which were measured at 10 and 50 m depth, are shown in Table 2. The concentration of chl *a* and the abundance of all phytoplankton groups except the cryptophytes were in general positively correlated with the concentration of nutrients. The abundance of bacteria was in contrast not related to the nutrient concentration. The smaller virus groups (LFV and MFV) were negatively correlated and the larger viruses (HFV) positively correlated to the concentration of nutrients. Assuming that the HFV are dominated by large algal viruses one possible explanation for the latter correlations may be that viral activity depends on growth and nutrient status of their phytoplankton hosts, which in turn depends on the availability of nutrients. The strong negative correlation between LFV, which presumably are dominated by bacteriophages, and nutrients may be explained assuming that high nutrient concentration and nutrient replete phytoplankton excrete less dissolved organic material (DOM) to support bacterial growth and virus production, while low nutrient concentration and nutrient depleted phytoplankton excrete more DOM sustaining bacterial growth and virus production. The N/P ratio had in most cases no impact although the N/P ratio at 10 and 50 m depth was significantly different ( $6.8 \pm 3.7$  vs  $13.2 \pm 1.7$ , (mean  $\pm$  SD, *t*-test  $p < 0.001$ ).

In complex natural environments correlations between different groups of planktonic organisms may be notoriously difficult to interpret (e.g. Li et al., 2004; Sherr et al., 2006).

Without a model or an a priori reason, the interpretation of many correlations such as between certain phytoplankton and viral groups will also be inclined to pure speculation. The correlation between *Synechococcus* and high fluorescent viruses observed in this study is thus presumably due to covariance between several biological and environmental factors and not a

**Table 2**

Partial correlation controlling for depth between nutrients, chl *a* (*in situ* fluorescence) and population abundances obtained by flow cytometry at 10 and 50 m depth. The original data were replaced by their logarithms and each variable normalized to have 0 mean and SD of 1.

	Nitrate	Phosphate	Silicate	N/P-molar ratio
Chl <i>a</i>	0.150	0.445**	0.624***	-0.091
<i>Synechococcus</i>	0.464**	0.562***	0.580***	0.219
Autotrophic picoplankton	0.246	0.449**	0.509***	0.024
Cryptophytes	-0.079	0.210	0.208	-0.225
Autotrophic nanoflagellates	0.225	0.430**	0.469**	0.009
Bacteria	-0.125	-0.020	0.073	-0.139
Low Fluorescence Virus	-0.504***	-0.570***	-0.667***	-0.262
Medium Fluorescence Virus	-0.483**	-0.340*	-0.426**	-0.379*
High Fluorescence Virus	0.380*	0.261	0.347*	0.302

\*  $p < 0.05$ .

\*\*  $p < 0.01$ .

\*\*\*  $p < 0.001$ .

manifestation of biological processes and connections. The same may be true for many of the other statistically significant correlations observed here (Tables 1 and 2) as well as in other studies.

### 3.9. Concluding remark

In this descriptive study we have explored the diversity and variation of the plankton community in Skagerrak and Norwegian coastal waters using a variety of different methods.

Including the smallest plankton forms i.e. picoplankton, *Synechococcus* bacteria and virus abundance, the picture emerging from this study is far more comprehensive than provided by earlier surveys in the region. Employing a range of complementary methods we find that the results agree and conclude that we do not seem to lose or overlook important parts of the phytoplankton community. Adding rate measurements to assess activities and molecular methods to resolve the diversity of the picoplankton, bacteria and viruses would have consolidated the study, but to understand the dynamics of the system we need seasonal studies to cover temporal variations and long term changes.

### Acknowledgments

We wish to thank UiB for granting ship time and the crew of research vessel Håkon Mosby cruise 0111 for companionship and assistance. Thanks to Dr. Anton Korosov at the Nansen Center for processing the satellite images. The research was funded by The Research Council of Norway (Project no. 121425/420) and the European Research Council Advanced Grant project No. 250254 “MINOS”. SJ was granted by an individual postdoctoral Marie Curie fellowship (HPMF-CT-1999-00030).

### Appendix A. Supplementary materials

Supplementary data associated with this article can be found in the online version at [doi:10.1016/j.csr.2011.06.014](https://doi.org/10.1016/j.csr.2011.06.014).

### References

- Backe-Hansen, P., Thronsdon, J., 2002a. Pico- and nanoplankton from the inner Oslofjord, Eastern Norway, including description of two new species of *Luffisphaera* (*incerta sedis*). *Sarsia* 87, 55–64.
- Backe-Hansen, P., Thronsdon, J., 2002b. Occurrence of pico- and smaller nanoplanktonic flagellates in the inner Oslofjord, Eastern Norway, during the breeding season of the blue mussel (*Mytilus edulis* L.). *Sarsia* 87, 65–74.
- Banase, K., 1977. Determining the carbon-to-chlorophyll ratio of natural phytoplankton. *Mar. Biol.* 41, 199–212.
- Bell, T., Kalf, J., 2001. The contribution of picophytoplankton in marine and freshwater systems of different trophic status and depth. *Limnol. Oceanogr.* 46, 1243–1248.
- Bird, R.T., Kalf, J., 1984. Empirical relationships between bacterial abundance and chlorophyll concentration in fresh and marine waters. *Can. J. Fish. Aquat. Sci.* 41, 1015–1023.
- Braarud, T., Nygaard, I., 1980. Phytoplankton observations in offshore Norwegian coastal waters between 62°N and 69°N. 2. Diatom societies from Møre to Vesterålen, March–April 1968–1971. *Sarsia* 65, 93–114.
- Braarud, T., Gaarder, K.R., Nordli, O., 1958. Seasonal changes in the phytoplankton at various points off the Norwegian West Coast. *Fisk-dir. Havunders.* 12, 1–77.
- Bratbak, G., Levasseur, M., Michaud, S., Cantin, G., Fernández, E., Heimdal, B.R., Heldal, M., 1995. Viral activity in relation to *Emiliana huxleyi* blooms: PRIVATE a possible mechanism of DMSP release? *Mar. Ecol. Prog. Ser.* 128, 133–142.
- Bratbak, G., Heldal, M., Norland, S., Thingstad, T.F., 1990. Viruses as partners in spring bloom microbial trophodynamics. *Appl. Environ. Microbiol.* 56, 1400–1405.
- Brussaard, C., 2004. Optimization of procedures for counting viruses by flow cytometry. *Appl. Environ. Microbiol.* 70, 1506–1513.
- Caron, D.A., 1983. Technique for enumeration of heterotrophic nanoplankton using epifluorescence microscopy and comparison with other procedures. *Appl. Environ. Microbiol.* 46, 491–498.
- Dahl, E., Johannessen, T., 1998. Temporal and spatial variability of phytoplankton and chlorophyll *a*: lessons from the south coast of Norway and the Skagerrak. *ICES J. Mar. Sci.* 55, 680–687.
- Diez, B., Pedrós-Alió, C., Massana, R., 2001. Study of genetic diversity of eukaryotic picoplankton in oceanic regions by small-subunit rRNA gene cloning and sequencing. *Appl. Environ. Microbiol.* 67, 2932–2941.
- Dolan, J.R., Šimek, K., 1999. Diel periodicity in *Synechococcus* populations and grazing by heterotrophic nanoflagellates: analysis of food vacuole contents. *Limnol. Oceanogr.* 44, 1565–1570.
- Erga, S.R., Heimdal, B.R., 1984. Ecological studies on the phytoplankton of Korsfjorden, western Norway. The dynamics of a spring bloom seen in relation to hydrographical conditions and light regime. *J. Plankton Res.* 6, 67–90.
- Espeland, G., Thronsdon, J., 1986. Flagellates from Kilsfjorden, southern Norway, with description of two new species of Choanoflagellida. *Sarsia* 71, 209–226.
- Folkestad, A., Pettersson, L.H., Durand, D., 2007. Inter-comparison of ocean colour data products during algal blooms in the Skagerrak. *Int. J. Remote Sensing* 28, 569–592.
- Gasol, J.M., Duarte, C.M., 2000. Comparative analyses in aquatic microbial ecology: how far do they go? *FEMS Microb. Ecol.* 31, 99–106.
- Geider, R.J., MacIntyre, H.L., Kana, T.M., 1997. Dynamic model of phytoplankton growth and acclimation: responses of the balanced growth rate and the chlorophyll *a*:carbon ratio to light, nutrient-limitation and temperature. *Mar. Ecol. Prog. Ser.* 148, 187–200.
- Grebecki, A., 1962. Adsorption des fluorochromes par le cystome des Cillies. *Bull. Acad. Pol. Sci.* 10, 483–485.
- Heldal, M., Bratbak, G., 1991. Production and decay of viruses in marine waters. *Mar. Ecol. Prog. Ser.* 72, 205–212.
- Hobbie, J.E., Daley, R.J., Jasper, S., 1977. Use of nucleopore filters for counting bacteria by fluorescence microscopy. *Appl. Environ. Microbiol.* 33, 1225–1228.
- Jacquet, S., Heldal, M., Iglesias-Rodriguez, D., Larsen, A., Wilson, W., Bratbak, G., 2002. Flow cytometric analysis of an *Emiliana huxleyi* bloom terminated by viral infection. *Aquat. Microb. Ecol.* 27, 111–124.
- Jiang, S.C., Paul, J.H., 1994. Seasonal and diel abundance of viruses and occurrence of lysogeny/bacteriocinogeny in the marine environment. *Mar. Ecol. Prog. Ser.* 104, 163–172.
- Korosov, A.A., Pozdnyakov, D.V., Folkestad, A., Pettersson, L.H., Sørensen, K., Shuchman, R., 2009. Semi-empirical algorithm for the retrieval of ecology-relevant water constituents in various aquatic environments. *Algorithms* 2, 470–497.
- Lange, C.B., Hasle, G.R., Syvertsen, E.E., 1992. Seasonal cycle of diatoms in the Skagerrak, North Atlantic, with emphasis on the period 1980–1990. *Sarsia* 77, 173–187.
- Larsen, A., Fønnes, A., Sandaa, R.-A., Casberg, T., Thyrrhaug, R., Erga, S.R., Jacquet, S., Bratbak, G., 2004. Spring phytoplankton bloom dynamics in Norwegian coastal waters: microbial community succession and diversity. *Limnol. Oceanogr.* 49, 180–190.
- Li, W.K.W., Head, E.J.H., Harrison, W.G., 2004. Macroecological limits of heterotrophic bacterial abundance in the ocean. *Deep-Sea Res. Part I* 51, 1529–1540.
- Liu, H., Probert, I., Uitz, J., Claustre, H., Brousseau, S., Frada, M., Not, F., de Vargas, C., 2009. Extreme diversity in noncalcifying haptophytes explains a major pigment paradox in open oceans. *Proc. Natl. Acad. Sci.* 106, 12803–12808.
- Liu, H., Suzuki, K., Minami, C., Saino, T., Watanabe, M., 2002. Picoplankton community structure in the subarctic Pacific Ocean and the Bering Sea during summer 1999. *Mar. Ecol. Prog. Ser.* 237, 1–14.
- Lovejoy, C., Massana, R., Pedrós-Alió, C., 2006. Diversity and distribution of marine microbial eukaryotes in the Arctic Ocean and adjacent seas. *Appl. Environ. Microbiol.* 72, 3085–3095.
- Maranger, R., Bird, J., 1995. Viral abundance in aquatic systems: a comparison between marine and fresh waters. *Mar. Ecol. Prog. Ser.* 121, 217–226.
- Marie, D., Brussaard, C.P.D., Bratbak, G., Vaulot, D., 1999. Enumeration of marine viruses in culture and natural samples by flow cytometry. *Appl. Environ. Microbiol.* 65, 45–52.
- Menden-Deuer, S., Lessard, E.J., 2000. Carbon to volume relationships for dinoflagellates, diatoms, and other protist plankton. *Limnol. Oceanogr.* 45, 569–579.
- Morel, A., Prieur, L., 1977. Analysis of variations in ocean colour. *Limnol. Oceanogr.* 22, 709–722.
- Mühling, M., Fuller, N.J., Millard, A., Somerfield, P.J., Marie, D., Wilson, W.H., Scanlan, D.J., Post, A.F., Joint, I., Mann, N.H., 2005. Genetic diversity of marine *Synechococcus* and co-occurring cyanophage communities: evidence for viral control of phytoplankton. *Environ. Microbiol.* 7, 499–508.
- Not, F., Massana, R., Latasa, M., Marie, D., Colson, C., Eikrem, W., Pedrós-Alió, C., Vaulot, D., Simon, N., 2005. Late summer community composition and abundance of photosynthetic picoeukaryotes in Norwegian and Barents Seas. *Limnol. Oceanogr.* 50, 1677–1686.
- O'Reilly, J.E., Maritorena, S., Harding, L., Magnuson, S., Zibordi, G., 28–29 July 1999. Ocean chlorophyll 2 version 2. In: Proceedings of the SeaWiFS Postlaunch Algorithm Mini-Workshop, NASA/GSFC, Greenbelt, Maryland. <<http://seawifs.gsfc.nasa.gov/~sbailey/wkshp-main.html>>.
- Pozdnyakov, D.V., Korosov, A.A., Grassl, H., Pettersson, L.H., 2005. An advanced algorithm for operational retrieval of water quality parameters from satellite data in the visible. *Int. J. Remote Sensing* 26, 2669–2687.
- Rey, F., Noji, T.T., Miller, L.A., 2000. Seasonal phytoplankton development and new production in the central Greenland Sea. *Sarsia* 85, 329–344.
- Reid, P.C., Lancelot, C., Gieskes, W.W.C., Hagmeier, E., Weichart, G., 1990. Phytoplankton of the North Sea and its dynamics: a review. *Neth. J. Sea Res.* 26, 295–331.

- Rousseau, V., Mathot, S., Lancelot, C., 1990. Calculating carbon biomass of *Phaeocystis* sp. from microscopic observations. *Mar. Biol.* 107, 305–314.
- Sathyendranath, S., Stuart, V., Nair, A., Oka, K., Nakane, T., Bouman, H., Forget, M.-H., Maass, H., Platt, P., 2009. Carbon-to-chlorophyll ratio and growth rate of phytoplankton in the sea. *Mar. Ecol. Prog. Ser.* 383, 73–84.
- Sandaa, R.-A., Larsen, A., 2006. Seasonal variations in virus-host populations in Norwegian coastal waters: focusing on the cyanophage community infecting marine *Synechococcus* spp. *Appl. Environ. Microbiol.* 72, 4610–4618.
- Sherr, E.B., Sherr, B.F., Longnecker, K., 2006. Distribution of bacterial abundance and cell-specific nucleic acid content in the Northeast Pacific Ocean. *Deep-Sea Res. Part I* 53, 713–725.
- Sherr, E.B., Sherr, B.F., Wheeler, P.A., 2005. Distribution of coccoid cyanobacteria and small eukaryotic phytoplankton in the upwelling ecosystem off the Oregon coast during 2001 and 2002. *Deep-Sea Res. II* 52, 317–330.
- Škaloud, P., Řezáčová, M., Ellegaard, M., 2006. Spatial distribution of phytoplankton in spring 2004 along a transect in the eastern part of the North Sea. *J. Oceanogr.* 62, 717–729.
- Strickland, J.D.H., Parsons, T.R., 1972. A practical handbook of seawater analysis. *Fish. Res. Board Can. Bull.* 167 (second ed.).
- Suttle, C.A., Chan, A.M., 1994. Dynamics and distribution of cyanophages and their effect on marine *Synechococcus* spp. *Appl. Environ. Microbiol.* 60, 3167–3174.
- Thronsen, J., 1969. Flagellates of Norwegian coastal waters. *Norw. J. Bot.* 16, 161–216.
- Thronsen, J., 1976. Occurrence and productivity of small marine flagellates. *Norw. J. Bot.* 23, 269–293.
- Vaulot, D., Marie, D., 1999. Diel variability of photosynthetic picoplankton in the equatorial Pacific. *J. Geophys. Res.—Oceans* 104, 3297–3310.
- Veldhuis, M.J.W., Kraay, G.W., 2004. Phytoplankton in the subtropical Atlantic Ocean: towards a better assessment of biomass and composition. *Deep Sea Res. I* 51, 507–530.
- Waterbury, J.B., Valois, F.W., 1993. Resistance to co-occurring phages enables marine *Synechococcus* communities to coexist with cyanophages abundant in seawater. *Appl. Environ. Microbiol.* 59, 3393–3399.
- Weinbauer, M.G., 2004. Ecology of prokaryotic viruses. *FEMS Microb. Rev.* 28, 127–181.
- Weinbauer, M.G., Fuks, D., Puskaric, S., Peduzzi, P., 1995. Diel, seasonal, and depth-related variability of viruses and dissolved DNA in the Northern Adriatic Sea. *Microb. Ecol.* 30, 25–41.
- Winter, C., Herndl, G.J., Weinbauer, M.G., 2004. Diel cycles in viral infection of bacterioplankton in the North Sea. *Aquat. Microb. Ecol.* 35, 207–216.
- Wommack, K.E., Colwell, R., 2000. Virioplankton: viruses in aquatic ecosystems. *Microb. Mol. Biol. Rev.* 64, 69–114.
- Zhang, Y., Jiao, N., Hong, N., 2008. Comparative study of picoplankton biomass and community structure in different provinces from subarctic to subtropical oceans. *Deep-Sea Res. II* 55, 1605–1614.